Journal of Anatolian Environmental and Animal Sciences Year: 8, No: 4, 2023 (642-650)
(*Anadolu Çevre ve Hayvancılık Bilimleri Dergisi*)
DOI: https://doi.org/10.35229/jaes.1349826
JAES
AÇEH
Yıl: 8, Sayı: 4, 2023 (642-650)
ARAŞTIRMA MAKALESİ **RESEARCH PAPER**

Evaluation of Earthquake Impacts on Land Use and Land Cover (LU/LC) Using Google Earth Engine (GEE), Sentinel-2 Imageries, and Machine Learning: Case Study of Antakya

Neslisah CIVELEK[1,2] Melis İNALPULAT[2,3]* Levent GENC[2,4]
[1]*Çanakkale Onsekiz Mart University, School of Graduate Studies, Department of Geographical Information Technologies, 17020, Çanakkale, Türkiye*
[2]*Çanakkale Onsekiz Mart University, Computer-Agriculture-Environment-Planning (ComAgEnPlan) Study Group, 17020, Çanakkale, Türkiye*
[3]*Çanakkale Onsekiz Mart University, Faculty of Agriculture, Department of Agricultural Structures and Irrigation, Agricultural Remote Sensing Laboratory (AGRESEL), 17020, Çanakkale, Türkiye*
[4]*Çanakkale Onsekiz Mart University, Faculty of Architecture and Design, Department of Urban and Regional Planning, Land Use and Climate Change Laboratory (LUCCL) 17020, Çanakkale, Türkiye*

Geliş/Received: *29.08.2023* ***Kabul/Accepted:*** *22.09.2023* ***Yayın/Puplished:*** *31.12.2023*
How to cite: **Civelek, N. Inalpulat, M. & Genc, L. (2023).** Evaluation of Earthquake Impacts on Land Use and Land Cover (LU/LC) Using Google Earth Engine (GEE), Sentinel-2 Imageries, and Machine Learning: Case Study of Antakya. *J. Anatolian Env. and Anim. Sciences*, ***8***(4), 642-650. https://doi.org/10.35229/jaes.1349826
Atıf yapmak için: **Civelek, N. Inalpulat, M. & Genc, L. (2023).** Depremin Arazi Kullanım ve Arazi Örtüsü (AKAÖ) Üzerine Etkilerinin Google Earth Engine (GEE), Sentinel-2 Görüntüleri ve Makine Öğrenmesi Kullanılarak Değerlendirilmesi: Antakya Örneği. *Anadolu Çev. ve Hay. Dergisi*, ***8***(4), 642-650. https://doi.org/10.35229/jaes.1349826

*: https://orcid.org/0000-0001-7418-1666
: https://orcid.org/0009-0007-6077-7689
: https://orcid.org/0000-0002-0074-0987

***Corresponding author's:**
Melis INALPULAT
Çanakkale Onsekiz Mart University, Faculty of Agriculture, Department of Agricultural Structures and Irrigation, Agricultural Remote Sensing Laboratory (AGRESEL), 17020, Çanakkale, Türkiye,
✉: melissacan@comu.edu.tr

Abstract: Natural disasters, especially earthquakes, known to be the most devastating process that threating human life, ecosystems, and land properties including land use and land cover (LU/LC). Understanding of such changes may help for rehabilitation processes, as well as presentation of baseline to develop management strategies for further steps. Remote sensing technologies have long been used for determination of change directions and magnitudes after earthquakes while development in cloud-based platforms provided users to avoid issues in storage and processing costs, effectively. In present study, it was aimed to determine LU/LC changes occurred around Antakya city of Hatay after February 06, 2023 and February 20, 2023 earthquakes, which caused serious losses.It is important to understand the immediate and short-term changes after earthquake events in different scales whereby there was a lack for the spatial information in the area, and among different scales performance of 10 m pixel size was evaluated, which is widely used to obtain valuable informations on the alternations in land surface properties subsequent to such events. In addition to the overall changes, the changes within 5 km zone from central coordinates were also investigated by considering individual subzones with 1 km width. One of the most widely used machine learning algorithm, random forest (RF), was used classify Sentinel-2 imageries via Google Earth Engine (GEE) platform. Accuracy assessment procedures were implemented to determine reliabilities of LU/LC_{2022} and LU/LC_{2023}, and accuracies were found over 0.85. Investigation of overall changes have revealed that areas of forest (F) and cultivated fields (CF) were considerably decreased while concrete (C), natural vegetation (N) and water (W) areas have increased. Dispersal of collapse buildings resulted in increase of C class not only at city level, but also within each subzone of 5 km buffer zone. Classification of Sentinel-2 imageries through RF algorithm in GEE provided rapid and reliable results for determining changes in Antakya, may comprise a baseline for risk studies in the area, whereby periodically monitoring of further changes strongly suggested.

Keywords: Antakya, earthquake, GEE, LU/LC, machine learning, sentinel-2.

Depremin Arazi Kullanım ve Arazi Örtüsü (AKAÖ) Üzerine Etkilerinin Google Earth Engine (GEE), Sentinel-2 Görüntüleri ve Makine Öğrenmesi Kullanılarak Değerlendirilmesi: Antakya Örneği

Öz: Doğal afetler, özellikle depremler, insan hayatını, ekosistemleri, arazi kullanımı ve arazi örtüsü gibi arazi /özelliklerini tehdit eden en tahripkar süreçlerden biridir (AK/AÖ) . Buna benzer değişimlerin anlaşılması rehabilitasyon süreçlerine yardımcı olmanın yanında sonraki aşamalar için yönetim stratejileri geliştirilmesi açısından bir başlangıç noktası sağlar. Depremler sonrasında değişimin yönü ve büyüklüğünün belirlenmesinde uzaktan algılama teknolojileri uzun zamandır kullanılmakta olup, buluta dayalı platformların geliştirilmesi bu anlamda kullanıcıların depolama ve işleme maliyeti sorunlarından kaçınmasını etkili bir şekilde sağlamıştır. Bu çalışmada, ciddi kayıplara yol açan 6 Şubat 2023 ve 20 Şubat 2023 depremlerinden sonra Hatay iline bağlı Antakya'da meydana gelen AK/AÖ değişimlerinin belirlenmesi amaçlanmıştır. Depremlerin hemen ardından ve kısa dönemde gerçekleşen değişimlerin anlaşılması önemli olup, çalışma alanında yersel bilgilere ilişkin eksiklikler vardır ve farklı ölçekler arasından, afetler sonrasında arazi yüzeyi değişimlerinin belirlenmesinde önemli bilgiler

***Sorumlu yazar:**
Melis INALPULAT
Çanakkale Onsekiz Mart Üniversitesi, Ziraat Fakültesi, Tarımsal Yapılar ve Sulama Bölümü, Tarımsal Uzaktan Algılama Laboratuvarı (AGRESEL), 17020, Çanakkale, Türkiye
✉: melissacan@comu.edu.tr

elde edilmesinde yaygın olarak kullanılan 10 m piksel büyüklüğünün performansı değerlendirilmiştir. Bunun yanında, merkez koordinatlarından 5 km uzağı kapsayan zon içerisinde meydana gelen değişimler 1 km genişliğindeki alt zonlar gözetilerek incelenmiştir. Sentinel-2 görüntülerinin Google Earth Engine (GEE) ile sınıflandırılmasında en çok kullanılan makine öğrenmesi algoritmalarından bir olan rassal orman (RO) algoritması kullanılmıştır. AK/AÖ$_{2022}$ ve AK/AÖ$_{2023}$ güvenilirliklerinin belirlenmesi için doğruluk analizi prosedürleri uygulanmış, ve doğruluklar 0.85'in üzerinde bulunmuştur. Genel değişimlerin incelenmesi betonarme (B), doğal vejetasyon (D) ve su (S) alanların artarken orman (O) ve tarım (T) alanlarının dikkate değer şekilde azaldığını göstermiştir. Çöken binaların dağılışı yalnızca şehir düzeyinde değil, 5 km tampon zor içerisindeki herbir alt zon içerisinde B sınıf artışı ile sonuçlanmıştır. Sentinel-2 görüntülerinin RO algoritması ile GEE'nda sınıflandırılması Antakya'da meydana gelen değişimlerin belirlenmesinde hızlı ve güvenilir sonuçları vermiş olup, bölgede yapılacak risk çalışmaları için altlık teşkil edebilecektir ve gelecekteki değişimlerin periyodik olarak izlenmesi şiddetle önerilmiştir..

Anahtar kelimeler: AK/AÖ, Antakya, Deprem, GEE, Makine Öğrenmesi, Sentinel-2.

INTRODUCTION

Earthquakes are one of the most devastating disasters for many areas of the world. Severe earthquakes known to result in physical, economic, and social detriments in a certain area, which may significantly impact human life and activities (Ozyavuz et al., 2016; Yavasoglu and Varol Ozden, 2017). As it was mentioned by Ozcelik et al. (2023), preventing earthquake events is not possible while determination of vulnerable zones and considering the sensitivities in planning and management strategies provides avoiding from detrimental effects. Comprehensive and holistic approaches may help to minimize losses against such disasters, and may provide more dependable settlement areas, as well as more effective recovery process. On the other hand, rapid determination of the magnitude of the disaster has great importance. Moreover, monitoring of the post-disaster processes within periodical intervals may provide better understanding of the achievements in renewal and enhancement steps. As it was mentioned by Portillo and Moya, (2023), immediate determination of the earthquake damage presents the major challenge since rapid determination may help to increase survival rates by fastening the actions in the impacted area. In this context, remote sensing technologies present valuable tools and datasets not only in determining extents and recovery status of the impacted areas through land use and land use and land cover (LU/LC) (Joshi et al., 2021), but also for management of sources, disaster reliefs, and emergency regimes (Yan et al., 2018). There are various satellites and airborne systems consisted of different spectral, spatial, temporal and radiometric resolutions, which can be used for evaluating the amount of detriments all over the world. Among these satellite systems, Sentinel-2 provides a strong alternative by being free of charge, having relatively high spatial and temporal resolution. Moreover, different image processing software have developed for this purpose, whereby Google Earth Engine (GEE), one of the well-known cloud-based platforms, widely used for detection of changes in LU/LC statuses (Velastegui Montoya et al., 2022). In the last decades, use of machine learning algorithms for LU/LC classification became highly prevalent in different studies, whereby random forest (RF) reported to be most preferred algorithm in GEE-based studies (Amani et al., 2020), which is an ensemble method that combines many classification and regression trees (Breiman, 2001; Loukika, 2021).

Türkiye known to located within an important earthquake zone. Due to existence of active fault lines, the country cited to be highly fragile against quakes, and listed in high-risk category (Guner, 2020). Historical records have shown that various earthquakes have occurred in the known history, and caused death of thousands of people, together with serious financial losses. As it is well known, the most recent and destructive earthquakes occurred in Pazarcık (Mw7.7) and Elbistan (Mw7.6) districts of Kahramanmaraş Province on February 06, 2023, and in Hatay Province (Mw6.4) on February 20, 2023, caused over 50 thousand deaths, and great amount of property loss including more than 300 thousand collapsed buildings (Gokceoglu, 2023). Therefore, determination of the changes between impacted areas is significant. Different studies have conducted in the area using remote sensing techniques to determine the effects of earthquake in different aspects and purposes. For instance, a study was conducted within the impacted region from Kahramanmaraş Earthquakes for designating distribution of co-seismic surface raptures using high-resolution Maxar and GF-2 satellite data (Gao et al., 2023). Levin (2023) used nightly VIIRS Black Marble product of VNP46A1 to assess the impact of earthquake events on artificial nighttime lights in the same area. Yuan et al. (2023) examined the distribution of alternations in night time lights using daily data of NOAA-20 VIIRS NTL. Urban building damage in Kahramanmaraş was identified using Sentinel-1 data SAR change detection by Wang et al., (2023). An et al., (2023) used Sentinel-2 imageries for determination directions of horizontal deformation, and Sentinel-1 and ALOS-2 data for extracting the range and azimuth offsets to assess vertical change in the impacted area. Gkougkoustamos et al., (2023) determined ground deformation of the impacted area through Sentinel-2

imageries and image matching algorithm of normalized cross correlation.

The aim of present study is related to identification of the change in LU/LC status in one of the most impacted areas, Antakya city of Hatay Province, Türkiye using Sentinel-2 imageries and GEE platform. The changes in areas of main LU/LC classes, namely forest (F), water (W), cultivated fields (CF), concrete areas (C), and natural vegetation (N) were investigated in the whole district and within the 5 km zone around the city center to achieve the aim of the study.

MATERIAL AND METHOD

The study was conducted around centre of Antakya District, which is the second biggest district of Hatay Province, Türkiye, covering a survey area of 60 thousand ha. The central coordinates of the district are 36°14′40″N and 36°12′3″E. Typical Mediterranean Climate is dominant in the area, whereby the average annual temperatures range between 15.1°C and 20.0°C. Many agricultural products can grow in the area due to suitability of climate, together with soil and terrain conditions. On the other hand, the area has faced with three severe earthquake events in February, 2023. Reports have shown that more than 20 thousand people died, and over 55 thousand buildings collapsed as results of the earthquakes. Since the highest losses are occurred around the main settled area, the changes within 5 km buffer zone from the city center that consisted of individual subzones with 1 km intervals were also investigated to evaluate the change amounts in different parts of the residential areas. The area of 5 km zone was 7845 ha, while the subzone areas are ranged from 314 ha to 2825 ha, respectively (Table 1). The locations of Hatay and Antakya city centre in Turkey, and different zones with 1 km distance from each other have shown in Figure 1.

Table 1. Properties of investigated zone/subzones.

Zone Code	Coverage (km)	Survey Area (ha)
0-5	0-5 km	7845
1st	0-1 km	314
2nd	1-2 km	941
3rd	2-3 km	1569
4th	3-4 km	2196
5th	4-5 km	2825

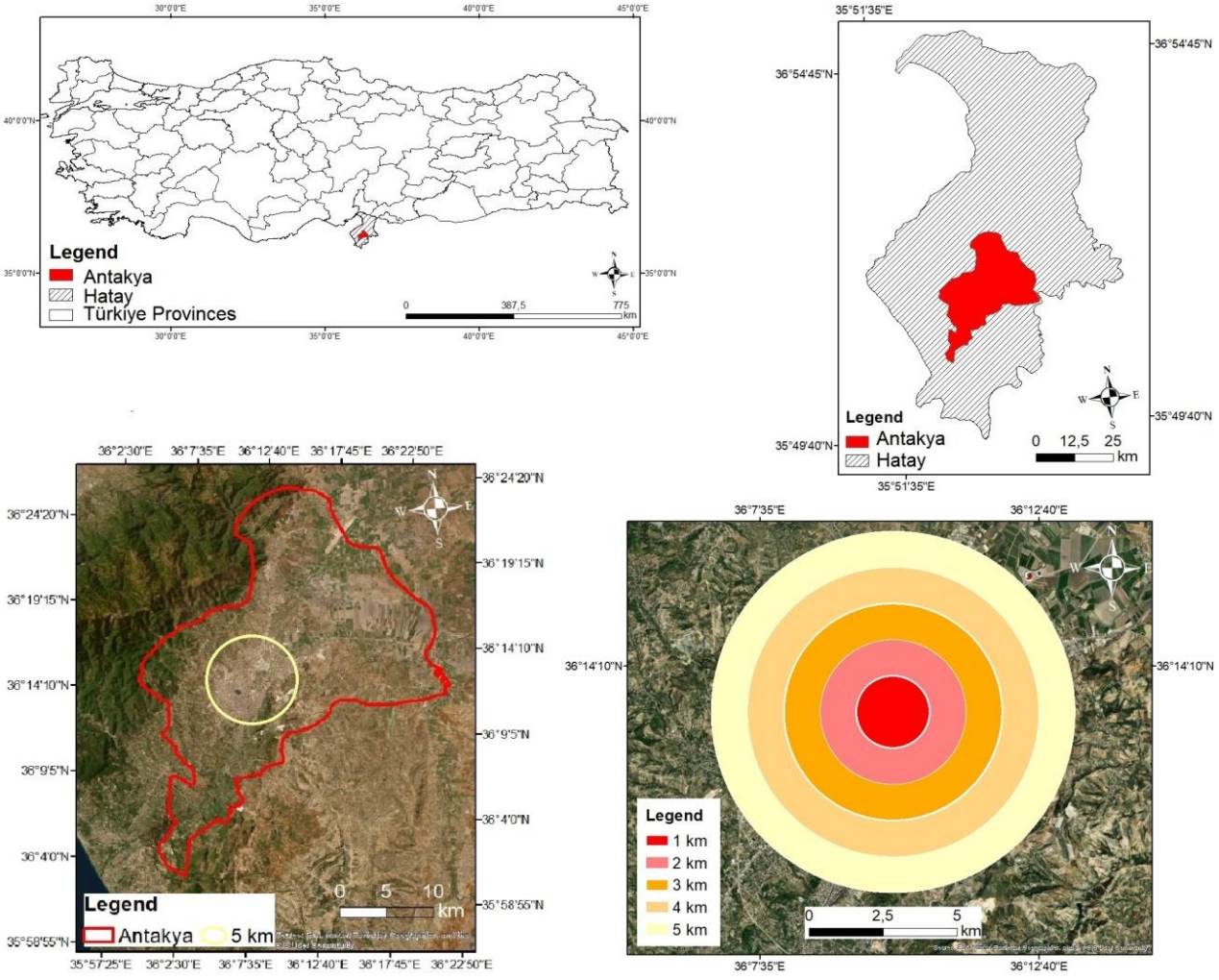

Figure 1. Location of 5 km zone around city center in Antakya District, Hatay Province, Turkey

Satellite Data: Sentinel-2 imageries were used as the main data in the study, which have 13 bands covering different regions of electromagnetic spectrum at different spatial resolutions. The images were selected depending on the acquisition month of different years to ensure similar conditions for avoiding the effects that may source from different illumination, cultivation pattern and climate conditions. The cloud cover threshold was determined as 20%. Pre-earthquake LU/LC status was evaluated through March 16, 2022 imagery. Meanwhile, post-earthquake LU/LC status was determined using the image acquired on March 11, 2023. The visible, near-infrared, and shortwave-infrared bands were used in the study.

Image Processing, Classification and Accuracy Assessment: Prior to the classification, the spatial resolutions of used bands were fixed at 10 m through resampling method. The RF algorithm, one of the most widely used machine learning algorithms for classification, was used to obtain LU/LC maps to evaluate pre-earthquake (LU/LC_{2022}) and post-earthquake (LU/LC_{2022}) statuses of Antakya District. Five main LU/LC types were considered including F, W, CF, C, and N classes. Training samples were collected from each class to implement RF classification procedures through GEE.

Subsequent to the classification, accuracy assessments were conducted using randomly selected reference points (Table 2). The overall accuracy (OA) and overall kappa (OK) values were calculated. In addition to OA (Eq. 1) and OK (Eq. 2), user's accuracy (UA) (Eq. 3) and producer's accuracy (PA) (Eq. 4) of each class were also evaluated to be confident on the reliability of class level accuracies. Steps of the study has summarized as flowchart in Figure 2.

Table 2. Number of reference points for each LU/LC maps.

Class	LU/LC_{2022}	LU/LC_{2023}
F	164	146
W	173	140
CF	350	324
C	384	316
N	140	187
Total	1211	1113

$$OA = \frac{\sum NoCC_P}{\sum NoR_P} \times 100 \quad \text{(Eq. 1)}$$

$$OK = \frac{P_0 - P_C}{1 - P_C} \quad \text{(Eq. 2)}$$

$$UA = \frac{\sum NoCC_{PLULC}}{\sum NoR_{PLULC}} \times 100 \quad \text{(Eq. 3)}$$

$$PA = \frac{\sum NoCC_P}{\sum NoC_{PLULC}} \times 100 \quad \text{(Eq. 4)}$$

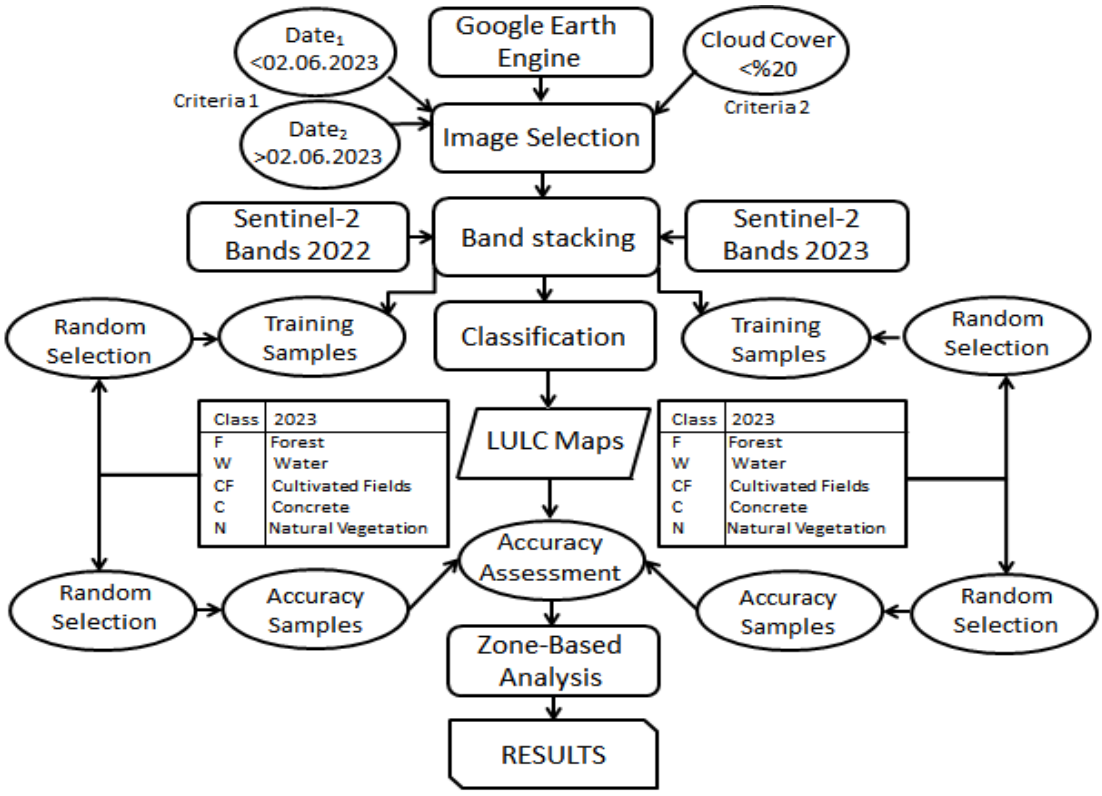

Figure 2. Implemented steps in the study.

RESULTS

Accuracy of Produced Maps: As it is well documented in many studies, K values known to range between 0-1 (Cohen, 1960), and categorized in different agreement levels by Landis and Koch, (1977). Accordingly, 0.00-0.20 indicates slight agreement, 0.21-0.40 represents fair agreement, 0.41-0.60 designates

moderate agreement, 0.61-0.80 shows substantial agreement, and 0.81–1.00 presents almost perfect agreement levels, respectively. In another point of view, accuracy values over threshold of 0.75 denoted to represent good classifications (Bharatkar and Patel, 2013). In present study, the OA and K values of LU/LC_{2022} were calculated as 0.88 and 0.85, respectively (Table 3). The OA and K of LU/LC_{2023} were slightly lower when compared to LU/LC_{2022} with values of 0.87 and 0.83 by the same order. Depending on the definitions of different K ranges, both pre- and post-earthquake LU/LC maps can be considered as almost perfect agreement level. Moreover, as it can be seen from Table 2, the UA and PA of each class were over the threshold value of 0.75 for pre-earthquake and post-earthquake LU/LC statuses of the area. Therefore, findings have demonstrated that the RF classifications were strongly reliable.

Overall LU/LC Changes: The term land use refers to how physical land features on Earth's surface are used by human, while land cover is defined as physical land features covering the earth surface like water bodies, forest, agricultural land (Anderson et al., 1976). The study considers both terms since natural disasters have great impact on both the use and cover of the land. The pre-earthquake and post-earthquake LU/LC statuses of the study area are given in Figure 3a and 3b, respectively. Visual analysis has shown that there are noticeable alternations in classes. The most probable reasons for such changes in cities have reported to arise from exploit of population, lack of coordination, and improper developments in infrastructure (Balamurugan and Aravind, 2015). As it was noted by Demirkesen, (2012), the area is one of the most precise coastal ecosystem areas against earthquakes, covered by fertile plains, erosion induced mountains, volcanic sedimentary and tectonic rock structures, which may help to understand the underlying reasons for magnitude of the changes.

Table 3. Accuracies and Kappa values of LU/LC_{2022} and LU/LC_{2023}.

Class	LU/LC_{2022}		LU/LC_{2023}	
	UA	PA	UA	PA
F	0.91	0.93	0.89	0.91
W	0.97	0.99	0.98	0.94
CF	0.79	0.89	0.80	0.81
C	0.93	0.87	0.93	0.93
N	0.90	0.77	0.73	0.74
OA	0.88		0.87	
OK	0.85		0.83	

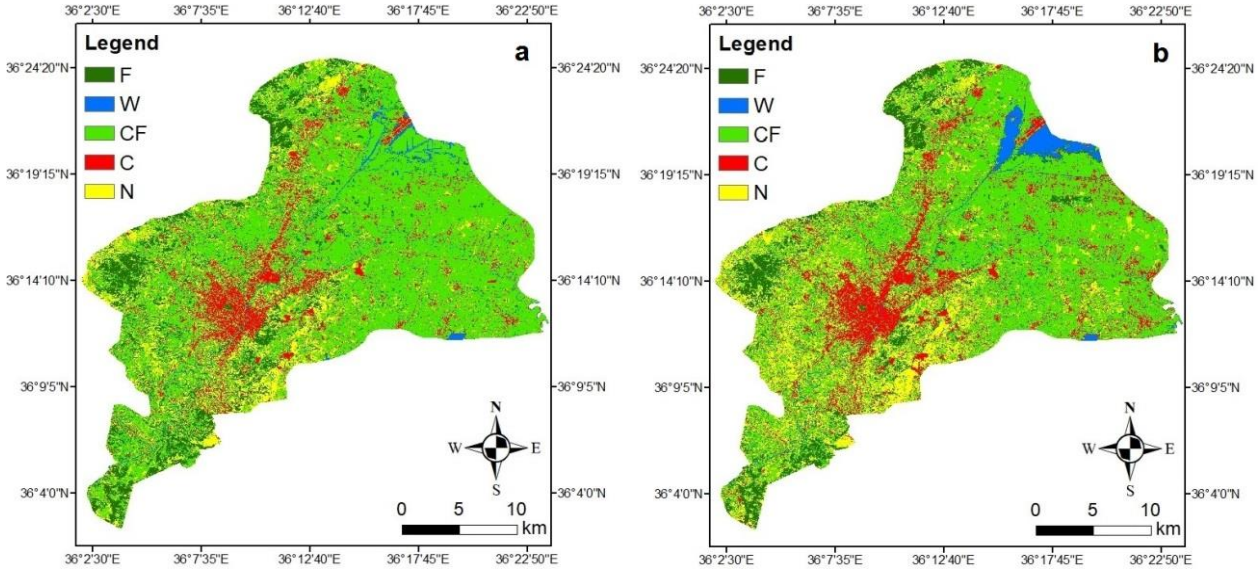

Figure 3. a. Pre-earthquake map (LU/LC_{2022}), and **b.** post-earthquake map (LU/LC_{2023}) including F (forest), W (water), CF (cultivated fields), C (concrete), and N (natural vegetation).

Depending on the LU/LC_{2022} and LU/LC_{2023}, the pre-earthquake and post-earthquake areas (ha) of each class, and the amount of change were calculated (Figure 4). The LU/LC_{2022} demonstrated that the majority of the area was covered by CF areas, and it was followed by F, N, C and W classes, respectively. The areas of W, C, and N classes were increased, while there were considerable decreases in F, and particularly, CF class. Therefore, the order of coverage area was altered as CF, N, C, F and W in the post-earthquake status of LU/LC_{2022}. Area of F class decreased from 8638 ha to 6890 ha with a reduction of 1748 ha. The change in the F areas sourced from fall of trees due to the severity of the disaster and some landslides, whereby comparable result was reported by Chen and Nhakatsugawa, (2021) in Japan. As another noticeable result, water has logged into agricultural lands in the northeastern part of the district due to increased water level after the earthquake, and thus, area of W class seemed to expand. The W area increased by 853 ha and reached to 1740, which was 887 in the same month of previous year, 2022. Similar situation for increased water level was reported by Yoshii et al., (2013), against the earthquakes in

Chile and Japan, which occurred in 2010 and 2011, respectively. On the other hand the C class seemed more dispersed and covering wider area in comparison with pre-earthquake status of 2022 as another conspicuous result of the disaster, which is caused by collapse of buildings, as well as transport of debris to other spaces out of the urbanized area, whereas C areas changed from 6355 ha to 8445 ha with an increase of 2100 ha. Furthermore, this transport process generally led to accumulation of refuse materials of collapse buildings on fertile lands, which reduces CF areas in return. As another important point for the CF areas, agricultural activities are probable to be impeded due to water damage of increased level, especially salty water (Roy et al., 2014). As one of the most observable situation the highest decrease amount seen in CF class areas with a reduction of 3592 ha that was 37583 ha before decreasing to 33991 ha. Conversely, a relative increase has occurred in areas of N class due to lack of cultivation and maintenance activities in some C areas, where the C pixels previously surrounded by N ones, as Lee et al., (2002) has mentioned similar situations in Korea. A considerable increase occurred in N class with 2388 ha, which was priory 8576 ha and reached to 10964 ha. The increase in N area can be connected to decrease in F areas as a result of earthquake (Chen and Nhakatsugawa, 2021).

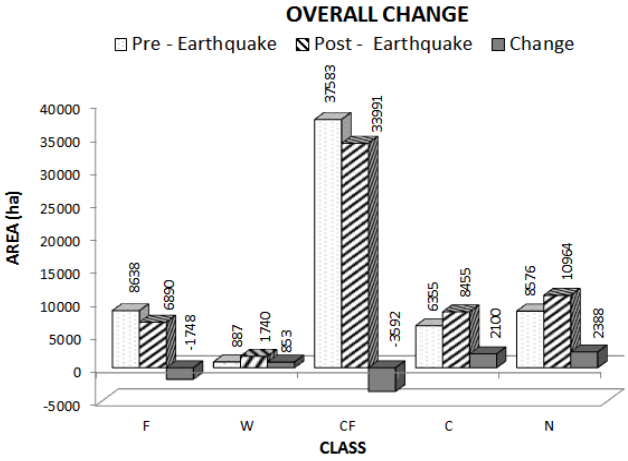

Figure 4. Overall changes in pre-earthquake and post-earthquake LU/LC statuses for F (forest), W (water), CF (cultivated fields), C (concrete), and N (natural vegetation).

LU/LC Changes in 0-5 km Zone and Subzones: The major LU/LC class in terms of coverage area seemed to be CF in the 0-5 km zone according to pre-earthquake status of LU/LC_{2022}, whereas C class comprised the seconder majority, and followed by N, F and W classes, respectively. However, post-earthquake LU/LC_{2023} status was quite different since the dispersion in C areas resulted in drastic increase in coverage of C, and became dominant in the area. Investigation of the changes within the zone between 0 and 5 km around the city centre has revealed that the directions of the changes in the LU/LC types were mostly similar to overall changes in Antakya, except the decreases in W (7 ha) and N (80 ha) class areas (Figure 5). Moreover, reduction of F and CF classes were 210 ha and 267 ha, respectively. In addition to the drastic changes in F and CF classes, the most remarkable change was the increase of C areas by 562 ha. The CF class presented main source for the new C areas in 0-5 km zone. However, a part of the C increase has potential to be sourced from actual expansion of the city within the one year period, particularly in the outer sites of 2022 year urban growth boundaries. Thence, for more precise investigation of earthquake-related changes around the settled areas, changes were evaluated considering individual subzones with 1 km intervals in the further steps (Figure 6a-e).

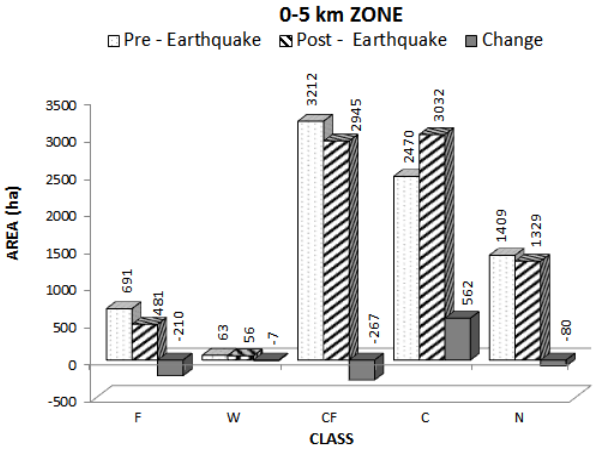

Figure 5. The changes in 0-5 km zone of pre-earthquake and post-earthquake LU/LC statuses for F (forest), W (water), CF (cultivated fields), C (concrete), and N (natural vegetation).

Figure 6-10 represents the LU/LC changes in different subzones around city center. Findings have demonstrated that major part of the 1st subzone, which involves 1 km distance from the central coordinates, was covered by C areas, which is an expected situation since the center of the subzone identical to coordinates of central Antakya. The C class coverage was followed by C, CF, N, F, and W class areas, respectively. In comparison to LU/LC_{2022}, the areas of F, W, CF, and N classes were decreased by 11 ha, 2 ha, 2 ha, and 23 ha in the 1st subzone, respectively. The increment in C class was 38 ha, simultaneously, while the increase has sourced from the dispersion of collapsed buildings. N class seemed to be comprised majority of recent C areas in 0-1 km subzone (Figure 6). The dominant class was C in the 2nd subzone that covering 1 km to 2 km apart from the central coordinates. The areas of C and CF were highly close to each other. When the changes are evaluated, similar situations have found with the 1st subzone. However, the amounts of decrease in CF and increase in C were more obvious with the values of 38 ha and 94 ha, respectively. Furthermore, F, W and N class areas were reduced by 17 ha, 2 ha and 38 ha, with the same order. Contrary to first

subzone, both CF and N classes were accounted for ne C areas with identical decrease amount (Figure 7). The order of class areas in 3rd subzone were coherent with the 2nd one in the pre-earthquake period, and stayed the same after the earthquake. On the other hand, the severity of reductions in F (24 ha), C (52 ha) and N (54 ha) classes was increased in the 3rd subzone, while C areas increased by 133 ha (Figure 8). The N class found to be the major source for new C areas within this subzone. Since the outer zones are more close to F, CF and N areas, the order of the area dominancy significantly alters from C to CF classes in the 4th subzone of LU/LC_{2022}. However, C class became dominant in LU/LC_{2023}. The change in C class has the highest value with 156 ha, while decreases in F, W, C, and N classes were 55 ha, 1 ha, 102 ha, and 2 ha, respectively, whereby majority of new C areas were converted from CF class (Figure 9). Finally, there were reductions in F (103 ha), W (1 ha) and CF (73 ha) classes, whereas areas of C and N classes were increased by 141 ha and 35 ha, respectively. Together with F areas, CF presented new places for C and N areas in the subzone (Figure 10).

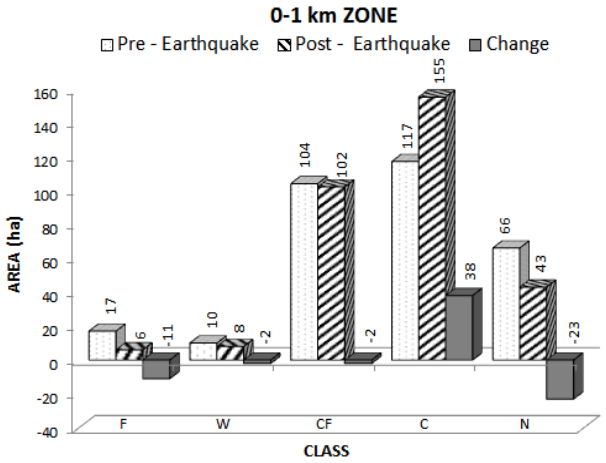

Figure 6. The changes in 0-1 km zone of pre-earthquake and post-earthquake LU/LC statuses for F (forest), W (water), CF (cultivated fields), C (concrete), and N (natural vegetation).

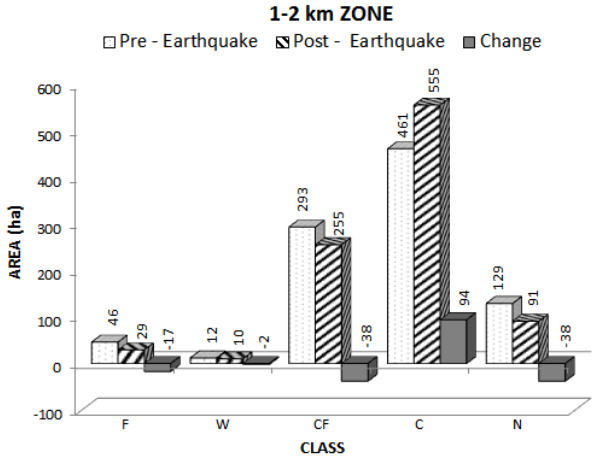

Figure 7. The changes in 1-2 km zone of pre-earthquake and post-earthquake LU/LC statuses for F (forest), W (water), CF (cultivated fields), C (concrete), and N (natural vegetation).

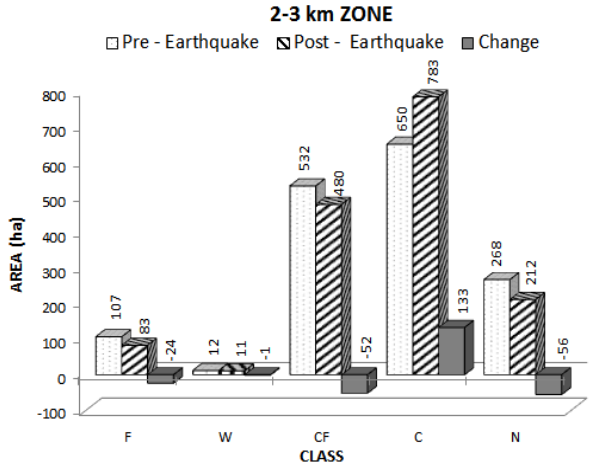

Figure 8. The changes in 2-3 km zone of pre-earthquake and post-earthquake LU/LC statuses for F (forest), W (water), CF (cultivated fields), C (concrete), and N (natural vegetation).

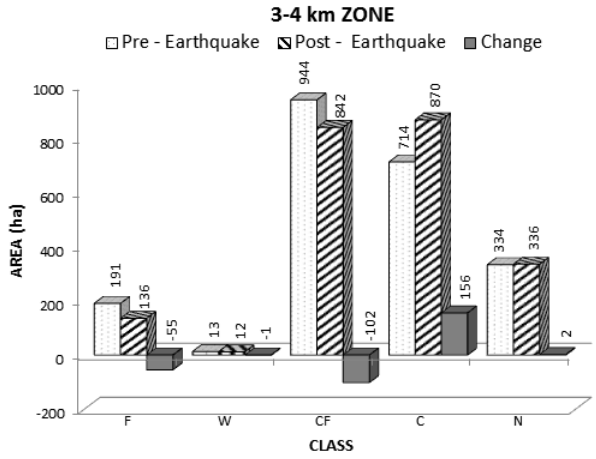

Figure 9. The changes in 3-4 km zone of pre-earthquake and post-earthquake LU/LC statuses for F (forest), W (water), CF (cultivated fields), C (concrete), and N (natural vegetation).

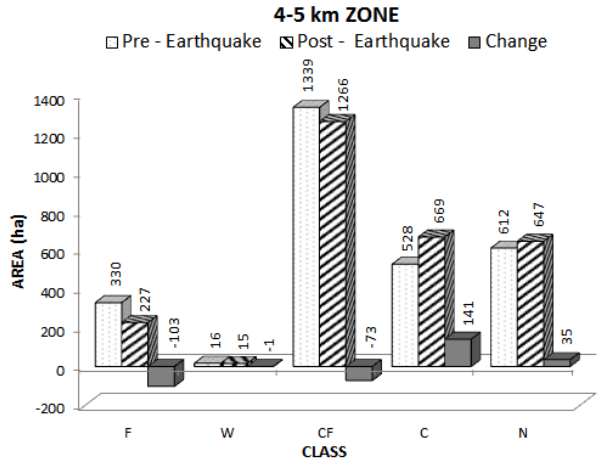

Figure 10. The changes in 4-5 km zone of pre-earthquake and post-earthquake LULC statuses for F (forest), W (water), CF (cultivated fields), C (concrete), and N (natural vegetation).

CONCLUSION

Present study aimed to investigate LU/LC changes in Antakya to assess the impacts of earthquake on LU/LC status within different buffer zones. Depending on

the accuracy results, it can be said that Sentinel-2 imageries can be reliably use for such purposes with high accuracy even under complex dispersal conditions, and using GEE enabled achieving more rapid change and accuracy results while reducing the efforts of labor and storage. Moreover, it was seen that the most observable change was the drastic decrease in CF class area in the city. In comparison, the increase in C areas within 0-5 km zone around the city center seemed more conspicuous. Evaluation of the changes in different subzones provided better understanding of the effects of collapsed buildings on different parts of the central area. Evaluating LU/LC changes after earthquake events provides linking complementary points of disaster management, sustainable development and durability goals. The rehabilitation of the area through socio-economic development can be promoted by adopting appropriate management strategies by considering the underlying reasons of the unforeseen destruction, while aiming the restoration of both human and ecology relate processes. In conclusion, the study believed to present a baseline for researchers from different disciplines, as well as local and regional authorities. However, continuous and more detailed monitoring of the area is strongly suggested to assess the rehabilitation processes for all ecosystems.

REFERENCES

Amani, M., Ghorbanian, A., Ahmadi, S.A., Kakooei, M., Moghimi, A., Mirmazloumi, S.M., Moghaddam, S.H.A., Mahdavi, S., Ghahremanloo, M., Parsian, S., Wu, Q. & Brisco, B. (2020). Google Earth Engine cloud computing platform for remote sensing big data applications: A comprehensive review. *IEEE J. Sel. Top. Appl. Earth Obs. Remote Sens.*, ***13***, 5326-5350.

An, Q., Feng, G., He, L., Xiong, Z., Lu, H., Wang, X. & Wei, J. (2023). Three-dimensional deformation of the 2023 Turkey Mw 7.8 and Mw 7.7 earthquake sequence obtained by fusing optical and SAR images. *Remote Sensing*, ***15***, 2656.

Balamurugan, G. & Aravind, S.M. (2015). Land use land cover changes in pre- and post-earthquake affected area using Geoinformatics-Western Coast of Gujarat, India. *Disaster Advances*, ***8***(4), 8313.

Bharatkar, P.S. & Patel, R. (2013). Approach to accuracy assessment tor RS image classification techniques. *International Journal of Scientific & Engineering Research*, ***4***(12), 79-86.

Breiman, L. (2001). Random forests. *Mach. Learn.*, ***45***, 5-32.

Chen, Y. & Makoto, N. (2021). Analysis of changes in land use/land cover and hydrological processes caused by earthquakes in the Atsuma River Basin in Japan. *Remote Sensing*, ***13***, 13041.

Cohen, J. (1960). A Coefficient of agreement for nominal scales. *Educational and Psychological Measurement*, ***20***, 37-46.

Demirkesen, A.C. (2012). Multi-risk interpretation of natural hazards for settlements of the Hatay province in the east Mediterranean Region,Turkey using SRTM DEM. *Environ. Earth Sci.*, ***65***, 1895-1907.

Gkougkoustamos, J., Krassakis, P., Kalogeropoulou, G. & Parcharidis, I. (2023). Correlation of ground deformation induced by the 6 February 2023 M7.8 and M7.5 earthquakes in Turkey inferred by Sentinel-2 and critical exposure in Gaziantep and Kahramanmaras cities. *GeoHazards*, ***4***, 267-285.

Gokceoglu, C. (2023). 6 February 2023 Kahramanmaraş - Türkiye earthquakes : A general overview. *The International Archives of the Photogrammetry, Remote Sensing and Spatial Information Sciences, Volume XLVIII-M-1-2023 39th International Symposium on Remote Sensing of Environment (ISRSE-39) "From Human Needs to SDGs",* 24-28 April 2023, Antalya, Türkiye, 417-424.

Gou, Y., Li, H., Liang, P., Xiong, R., Chaozhong, H. & Xu, Y. (2023). Preliminary report of coseismic surface rupture (part) of Turkey's MW7.8 earthquake by remote sensing interpretation. *Earthquake Research Advances*, 100219. DOI: 10.1016/j.eqrea.2023.100219

Guner, B. (2020). A periodical approach to earthquake damages in Turkey; 3 periods, 3 earthquakes. *Eastern Geographical Review*, ***25***(43), 139-152.

Joshi, G., Natsuaki, R. & Hirose A. (2021). Multi-sensor satellite-imaging data fusion for earthquake damage assessment and the significant features. *7th Asia-Pacific Conference on Synthetic Aperture Radar (APSAR)*. 1 November 2021, 1-6.

Landis, J.R. & Koch, G.G. (1977). The measurement of observer agreement for categorical data. *Biometrics*, ***33***(1), 159-174.

Lee, C.S., You, Y.H. & Robinson, G.R. (2002). Secondary succession and natural habitat restoration in abandoned rice fields of central Korea. Restor. Ecol., ***10***, 306-314.

Levin, N. (2023). Using night lights from Space to assess areas impacted by the 2023 Turkey earthquake. *Remote Sensing*, ***15***, 2120.

Loukika, K.N., Keesara, V.R. & Sridhar, V. (2021). Analysis of land use and land cover using machine learning algorithms on Google Earth Engine for Munneru River Basin, India. *Sustainability*, ***13***, 13758.

Ozcelik, A.E., Corbaci, O.L. & Yuksek, T. (2023). Spatial analysis of green areas located in affected cities by the Kahramanmaras centered earthquake according to earthquake susceptibility with Geographical Information Systems. *Journal of Anatolian Environmental and Animal Sciences*, ***8***(3), 273-282.

Ozyavuz, M., Donmez, Y. & Corbaci, O.L. (2016). Natural disaster management availability of open

and green areas; example of earthquake park. *Doğal Afet ve Afet Yönetimi Sempozyumu (DAAYS'16)*, 2-4 Mart 2016, Karabük, Türkiye.

Portillo, A. & Moya, L. (2023). Seismic risk regularization for urban changes due to earthquakes: A case of study of the 2023 Turkey earthquake sequence. *Remote Sens.*, ***15***, 2754.

Roy, K., Sasada, K. & Kohno, E. (2014). Salinity status of the 2011 Tohoku-oki tsunami affected agricultural lands in Northeast Japan. *International Soil and Water Conservation Research*, ***2***(2), 40-50.

Velastegui Montoya, A., Rivera Torres, H., Herrera Matamoros, V., Sades, L. & Pacheco Quevedo, R. (2022). Application of Google Earth Engine for land cover classification in Yasuni National Park, Ecuador. *International Geoscience and Remote Sensing Symposium*, 17-22 July 2022, Kuala-Lumpur, Malaysia, 6376-6379.

Vizzari, M. (2022). Planetscope, Sentinel-2, and Sentinel-1 data integration for object-based land cover classification in Google Earth Engine. *Remote Sensing*, ***14***(11), 2628.

Yan, Z., Huazhong, R. & Desheng, C. (2018). The research of building earthquake damage object-oriented change detection based on ensemble classifier with remote sensing image. *Geoscience and Remote Sensing Symposium,* 22-27 July 2018, Valencia, Spain, 4950-4953.

Yavasoglu, F. & Varol Ozden C.(2017). Using geographic information systems (GIS) BASED analytic hierarchy process (AHP) earthquake damage risk analysis: Kadikoy case. *Turkish Science Research Foundation,* ***10***(3), 28-38.

Yuan, Y., Wang, C., Liu, S., Chen, Z., Ma, X., Li, W., Zhang, L. & Yu, B. (2023). The changes in nighttime lights caused by the Turkey–Syria earthquake using NOAA-20 VIIRS Day/Night band data. *Remote Sensing*, ***15***, 3438.

Yoshii, T., Imamura, M., Matsuyama, M., Koshimura, S., Matsuoka, M., Mas, E. & Jimenez, C. (2012). Salinity in soils and tsunami deposits in areas affected by the 2010 Chile and 2011 Japan Tsunamis. *Pure and Applied Geophysics*, ***170***(6-8), 1047-1066.